

LUNAR DOMES NEAR MENELAUS CRATER. R. Evans¹, R. Lena², J. Phillips³, C. Wöhler⁴ – Geologic Lunar Research (GLR) group. ¹114 Simonds St., Fitchburg, MA 01420, USA, revans_01420@yahoo.com; ²Via Cartesio 144, sc. D, I-00137 Rome, Italy, r.lena@sanita.it; ³101 Bull Street, Charleston, SC 29401, USA, thefamily90@hotmail.com; ⁴Image Analysis Group, Dortmund University of Technology, Dortmund, Germany, christian.woehler@tu-dortmund.de

Introduction: The Menelaus region is located near the southern border of Mare Serenitatis (cf. Figs. 1 and 2). The Menelaus rilles occur along the crest of an elongated low ridge or bulge and were presumably formed when the load of younger mare lavas in the centre of the Serenitatis basin caused crustal subsidence and fractures at the mare edges. According to [1], two separate lava flows can be delineated, where the superposition by younger units occurred at the dome Menelaus 1 (termed Menelaus ζ in [1]) and younger lava surrounded an “inlier” of the old basalt covering part of the broad rille that bisects the inlier.



Figure 1: Upper left: Telescopic image acquired on November 08, 2009, at 08:05 UT. Top right: Image simulated based on the LOLA DEM using LTVT, assuming the same illumination conditions as in the telescopic image. Bottom left: Dome Menelaus 1 (Selene image at 1000 nm). Bottom right: Dome Menelaus 2 (Selene image at 1049 nm). Menelaus 1 is the western and Menelaus 2 the eastern dome. For all images, north is to the top and west to the left.

dome	flank slope [°]	D [km]	h [m]	V [km ³]
Menelaus 1	1.6	10 x 16	180	11.2
Menelaus 2	0.9	13 x 16	110	8.9

Table 1: Morphometric properties of the examined domes.

At a later time, a second eruptive stage occurred which covered the earlier lavas, leaving elevated terrain which appears darker in the Clementine 750 nm imagery and smoother along the northern and western end where the young lava curves around the older rise. The two domical structures might also be considered “mare kipukas”. It will

be shown that the surface along the broad fractures consists of a fairly untypical mare basalt.

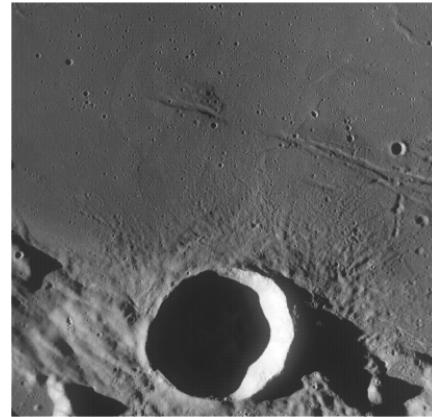


Figure 2: LRO WAC image M117386175ME.

Morphometric and rheologic properties: Based on the telescopic CCD image we obtained digital elevation maps (DEMs) of the examined domes by applying the combined photoclinometry and shape from shading method described in [2]. The heights of the domes were determined to 180 ± 20 m and 110 ± 10 m, resulting in flank slopes of $1.6^\circ \pm 0.2^\circ$ and $0.9^\circ \pm 0.1^\circ$, respectively (Table 1). If we assume an effusive volcanic origin for the two domes, the rheologic model introduced in [3] yields high effusion rates of 225 and 481 $\text{m}^3 \text{s}^{-1}$ for Menelaus 1 and 2. They were formed from lava of viscosities of 1.3×10^6 and 9.1×10^4 Pa s over a period of time of 1.6 and 0.6 years, respectively. The inferred rheologic properties are comparable to those of the class C₂ domes in the Cauchy region in Mare Tranquillitatis such as Cauchy ω and τ [2], and to the dome Kepler 1 [4]. According to the dike model introduced in [5], we estimated for the dome Menelaus 1 a magma rise speed of $U = 2.5 \times 10^{-5} \text{ m s}^{-1}$, a dike width of 47 m, and a dike length of 188 km. For the dome Menelaus 2, the estimated magma rise speed amounts to $U = 4.4 \times 10^{-4} \text{ m s}^{-1}$ and the dike width and length to 16 m and 70 km, respectively. These modelling results were obtained assuming a vertical magma pressure gradient of 328 Pa m^{-1} , the value inferred in [6] as the minimum value required for magma to ascend from the bottom of the lunar crust and erupt onto the surface. The dike lengths resulting from the model are comparable to the extension of the linear rilles associated with the two domes, which corresponds to about 100–150 km, suggesting that the Menelaus rilles may well represent the surface manifestations of dome-forming dikes.

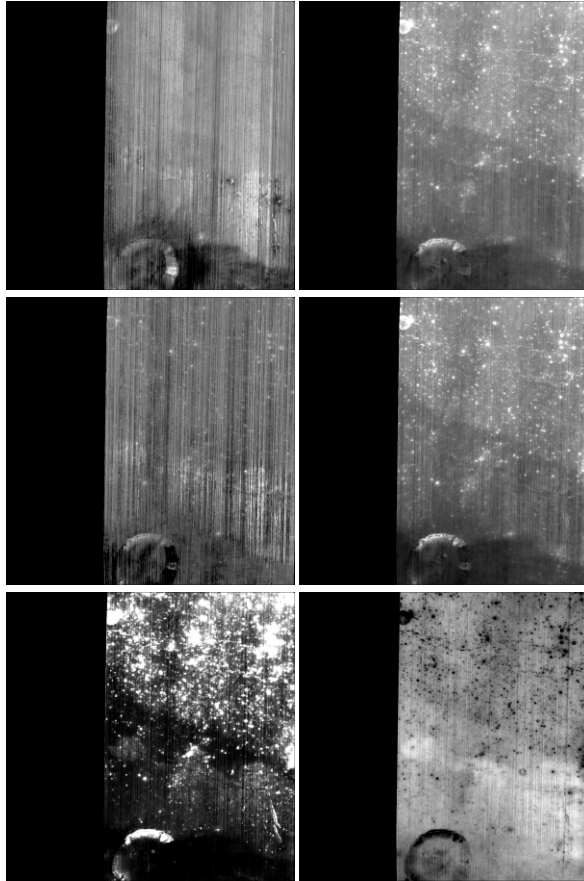


Figure 3: Spectral feature maps inferred from Chandrayaan-1 M³ multispectral data (longitude range from 14° to 18° E, latitude range from 16° to 20° N). Row-wise from top left to bottom right: Absorption wavelength (grey scale interval 900–1000 nm), relative band depth of 1000 nm absorption after continuum removal (0–0.25), FWHM of 1000 nm absorption (150–350 nm), IBD of 1000 nm absorption after continuum removal (0–70), IBD of pyroxene absorption at ~2000 nm after continuum removal (0–10), spectral ratio R_{2018}/R_{1509} (1.15–1.45).

Spectral properties: For both domes, Clementine UVVIS spectral data indicate a R_{415}/R_{750} ratio of about 0.60 and furthermore reveal a 750 nm reflectance of $R_{750} = 0.09$ and a weak mafic absorption with $R_{950}/R_{750} = 1.06$, suggesting a high soil maturity.

Selene VIS+NIR imagery of the bisected domes from 749 nm to 1548 nm were normalized using the Mare Serenitatis 2 site at 18.7° N, 21.4° E longitude and calibrated using bidirectional reflectance corrected Keck 120 color spectral data for Mare Serenitatis 2. The continuum-removed spectra of the domes show a strong absorption trough at about 1000 nm with an inflection feature at 1049 nm likely due to the presence of an olivine component, which causes the FWHM value to increase.

These findings are supported by the spectral features inferred from 85-band Chandrayaan-1 M³ multispectral data. After applying a thermal correction to the

recently released radiance spectra, we performed a division by the wavelength-specific solar irradiance and smoothed the resulting reflectance spectrum by a spline. Based on the approach outlined in [7], we then inferred the absorption wavelength, relative band depth, FWHM, and integrated band depth (IBD) of the ferrous absorption trough at ~1000 nm as well as the IBD of the pyroxene absorption trough at ~2000 nm and the spectral ratio R_{2018}/R_{1509} (cf. Fig. 3).

The increased absorption wavelength, the broadened absorption trough near 1000 nm, and the increased R_{2018}/R_{1509} spectral ratio indicate the presence of olivine-bearing mare basalt [8] for the domes and the mare surface along the Menelaus rilles.

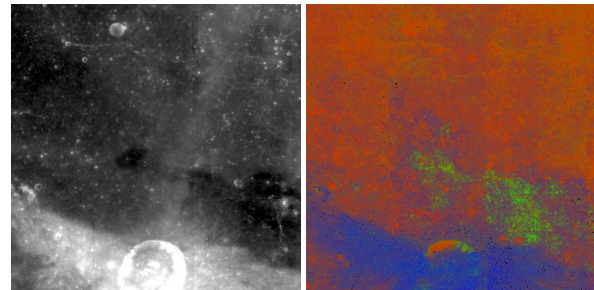


Figure 4: Left: Clementine 750 nm image of the Menelaus region. Right: Petrographic map.

Elemental abundances and petrographic analysis: We analysed the ~1000 nm absorption using Clementine UVVIS+NIR multispectral imagery according to [7], which allows a regression-based estimation of the abundances of the elements Ca, Al, Fe, Mg, Ti, and O based on the LP GRS elemental abundance data. Furthermore, we constructed a petrographic map which indicates the relative fractions of the three end-members mare basalt (red channel), Mg-rich rock (green channel), and ferroan anorthosite (FAN, blue channel). The region along the Menelaus rilles displays a high content of Mg-rich rock (cf. Fig. 4), which is again consistent with the presence of olivine.

Conclusion: We have examined two possible effusive domes bisected by linear rilles in terms of their morphometric and inferred rheologic properties and feeder dike dimensions. We have found that the region along the rilles consists of mare basalt with an unusually high olivine content.

References: [1] Howard K. A. et al. (1973) Apollo 17 Preliminary Science Report; [2] Wöhler et al. (2006) *Icarus* 183, 237–264; [3] Wilson L. and Head J. W. (2003) *JGR* 108(E2), 5012–5018; [4] Lena R. and Wöhler C. (2009) *LPSC XXXX*, Abstract #1092; [5] Rubin A. S. (1993) *Earth and Planet. Sci. Lett.* 199, 641–659; [6] Wilson L. and Head J. W. (1996) *LPSC XXVII*, Abstract #1445; [7] Wöhler C. et al. (2011) *Planet. Space Sci.* 59, 92–110; [8] King T. V. V. and Ridley W. I. (1987) *JGR* 92, 11457–11469.